

Theoretical mapping of interaction between alkali metal atoms adsorbed on graphene-like BC_3 monolayer

Kazem Zhou^a and Andrei Postnikov^a

^a LCP-A2MC Université de Lorraine 1 Bd Arago, F-57078 Metz Cedex 3, France

Corresponding authors emails: kazem.zhour@gmail.com; andrei.postnikov@univ-lorraine.fr

Abstract

First-principles calculations using density functional theory and two methods in comparison, Quantum ESPRESSO and SIESTA, are done on large supercells which describe different placements of two identical adsorbed alkali metal atoms (of either Na, or K species) on the monolayer of boron carbide BC_3 . The energy of single-atom adsorption over the center of C_6 ring, of the C_4B_2 hexagon and over a boron atom have been preliminarily estimated, the effect of applying the Grimme D2 correction on the adsorption characteristics evaluated, and the comparison of these results with available data discussed. The interaction of two identical Na or K atoms adsorbed at close enough distances (less than $\simeq 10$ Å) is negligible if the adsorption occurs at the opposite sides of the BC_3 layer, but creates a steep repulsive potential at distances less than $\simeq 8$ Å if both atoms are adsorbed on the same side of the monolayer. Relaxation patterns resulting from the two K atoms being trapped at adjacent adsorption sites in the lattice are explained. The results suggest that the density of adsorbed K atoms on BC_3 can be interestingly high.

Keywords: semiconductor; monolayer; alkali metal; adsorption; diffusion.

1 Introduction

Boron carbide (BC_3) recently emerged [1] as an interesting two-dimensional (2D) material, in its structure and some properties close to graphene, with the difference that its single layer is semiconducting and not semi-metallic. Certain expectations are related with using this material functionalized with metals, for so different purposes as alkali metal storage in batteries [2], enhanced sensibilisation for gas sensing [3], and hydrogen storage [4]. These lines of research brought about recent works of first-principles simulation, aimed at functionalisation of this material with adsorbed alkali metal atoms. Zhao *et al.* [5] probed different placements of Li, Na and K atoms over different sites of BC_3 , compared the corresponding adsorption energies, and traced the energy profiles across the barriers between adjacent adsorption sites. They used the VASP package on 3×3 supercells (of primitive cells with 2 formula units) and generalized gradient approximation for the exchange-correlation after the prescription of Perdew–Burke–Erznerhof (GGA-PBE) [6, 7]. Naqvi *et al.* [8] used the same calculation method (on a smaller, 2×2 supercell) to probe the docking of the same alkali metals and moreover of the alkaline earth metals, with subsequent adsorption

of CH₄, CO₂ and CO molecules at the metal sites. Bafekry *et al.* [9] explored different placements and estimated corresponding adsorption energies for a long list of adatoms and small molecules, in a series of calculations using OpenMX and SIESTA methods with GGA-PBE, for 2×2 supercell. All these studies, anticipating the importance of accounting for dispersion interactions in the study of the systems in question, included semiempirical D2 correction after Grimme [10].

Whereas these studies permit to provide some consistent idea of how would the alkali metal atoms place themselves onto, and diffuse over, the BC₃ layer, we find it interesting to address a hitherto unexplored issue of interaction of adsorbed atoms at the surface. This may help to parametrise this interaction to adequately model the diffusion, and/or to estimate maximal density of atoms to be placed on the surface, which may be helpful for the above discussed issues, i.e., battery electrodes or gas sensors. In view to probe this interaction, we considered supercells of larger size than in the mentioned previous studies, and decorated with two (identical) alkali metal atoms. Specifically, we studied K–K and Na–Na interactions. Two calculation methods have been used in comparison: SIESTA for principal large-size calculations and Quantum ESPRESSO for smaller-size benchmarks (including the Li adsorption as well, to this end). The calculation details are given in Section 2. We start with a short discussion of pristine BC₃ and the single-atom adsorption on it in Section 3, checking ourselves against the previous results, and come to novel results concerning interaction in Section 4. The conclusions are summarized in Sec. 5.

2 Calculation methods and technical details

We used two first-principles DFT methods in comparison, the plane-wave pseudopotential Quantum ESPRESSO (QE) [11, 12] and numerical orbitals pseudopotential SIESTA [13, 14]. Exchange-correlation was treated within the GGA, using the PBE parametrisation [6, 7]. SIESTA is generally expected to be more efficient than planewave methods in treating large open low-coordinated systems, but, at the same time, potentially sensitive to the “quality” of fixed basis functions adopted. After some tests, we found it sufficient to use double-zeta basis functions for all atoms, including notably $3p$ as a valence state for potassium. For sodium, the choice of the valence configuration for the construction of pseudopotential, namely, the attribution of Na $2p$ states (situated in a free atom at ~ -30 eV) either to valence states or to the core was not so obvious, since an accurate treatment of such semicore states may be essential for correct grasping of fine total-energy trends. Both cases have been tested. The pseudopotentials used were norm-conserving, generated according to the Trouiller – Martins scheme [15] for the following free-atom configurations (the cutoff radii in Bohr being indicated in parentheses for each l -channel) :
 K $4s^1(3.14) 3p^6(1.83) 3d^0(3.14) 4f^0(2.54)$, Na $3s^1(2.30) 2p^6(2.30) 3d^0(2.30) 4f^0(2.30)$ and Na $3s^1(2.83) 3p^0(2.83) 3d^0(3.13) 4f^0(3.13)$, B $2s^2(1.74) 2p^1(1.74) 3d^0(1.74) 4f^0(1.74)$, C $2s^2(1.54) 2p^2(1.54) 3d^0(1.54) 4f^0(1.54)$. The PA0.EnergyShift parameter in SIESTA was set to 0.015 Ry, that resulted in the maximal extension of basis functions of 5 Å.

In QE calculations, the kinetic energy and the charge density cutoffs were set to 50 Ry and 400 Ry, respectively. The convergence threshold for self-consistency in energy was set to 10^{-7} Ry. Ultrasoft pseudopotentials have been used with QE.

A $8\times 8\times 1$ undisplaced \mathbf{k} mesh was employed in electronic structure calculations for pristine BC₃, with appropriate reduction in larger supercells. The supercell “thickness” in

the slab geometry (i.e., the separation between periodically repeated BC_3 monolayers) was set at 30 Å, sufficient to exclude spurious interaction of adatoms with substrate across the vacuum layer, and to provide a reference “no interaction” energy of monolayer plus isolated atom when the latter was removed to the maximal distance (15 Å).

3 Pristine BC_3 and adsorption of alkali metals on it

Planar Boron carbide, described in Ref. [1], is characterized by a honeycomb planar lattice like that of graphene, in which one carbon atom out of four (equivalently, two atoms within a 2×2 graphene supercell) are substituted by boron. In principle, one can imagine different relative placements of B atoms on the honeycomb lattice, corresponding to para-, ortho- and meta-isomers (referred to as types A, B and C in Ref. [16]). However, the para-isomer is singled out by its more regular and symmetric arrangement in which every carbon atom has exactly one boron neighbour, and there are no B–B bonds. This isomer retains the hexagonal (super)structure, which makes a pattern of C_6 (perfect) hexagons with the C–C bond lengths $d_{\text{C-C}}\approx 1.4$ Å and C_4B_2 (distorted) hexagons around the perfect ones, with the C–B bond lengths $d_{\text{C-B}}\approx 1.6$ Å. The lattice parameter of this hexagonal unit cell which hosts two formula units is $a = \sqrt{3}(d_{\text{C-C}} + d_{\text{C-B}})$. Differently from perfect infinite graphene which has a zero gap, BC_3 has the band gap of 0.65 eV (in a single sheet). A summary of previous data concerning pristine BC_3 , along with our present results, is given in Table 1.

The works aimed at the study of alkali metal adsorption on BC_3 from first principles are not numerous. Understandably, the possible adsorption sites probed in previous works (notably Zhao *et al.*[5]) are over the center of one or another hexagon, over the C–C or C–B bonds, or over the one or the other atom species. Zhao *et al.* argued (with respect to Li, Na and K on BC_3 , which we could confirm, see below), that only three of these sites, over the both hexagons and atop a boron atom, emerge as local energy minima for adsorption.

There seems to be a consensus among the calculations done that the hollow site over the center of the C_6 hexagon, referred to as HC in the following, is the preferential one, closely followed by the hollow site over the center of the C_4B_2 hexagon, referred to as HB. With respect to the magnitudes of the adsorption energy, however, there seems to be a controversy we show in Table 2. We performed our calculations using sufficiently large supercell (in terms of B_2C_6 unit cells) per adsorption atom and inspected several possible sources of controversy. Without much details given in the papers cited, good “suspects” could be the basis set superposition error (BSSE, Ref. [18]), potentially dangerous in methods with

Table 1: Calculated properties of single-layer BC_3 .

Method	Ref.	$d_{\text{C-C}}$ (Å)	$d_{\text{C-B}}$ (Å)	a (Å)	E_{gap} (eV)
SIESTA GGA	present work	1.428	1.564	5.183	0.67
QE GGA	present work	1.421	1.564	5.170	0.51
VASP GGA	[17]	1.422	1.565	5.174	0.62
VASP GGA	[5]	1.42	1.57	5.17	0.66
SIESTA GGA	[9]	1.422	1.562	5.17	0.7

atom-centered basis functions (e.g., Ref. [9]), and the neglect of the magnetic state for an isolated potassium atom, both factors tending to overestimate the adsorption energy. Our result shown in Table 2 is obtained from comparing the energies of two sufficiently “thick” supercells of identical size, possessing the same 73 atoms: the relaxed system upon K adsorption, and the pristine BC₃ layer with the K atom removed away from the layer at a distance that would preclude the overlap of their basis functions. This does not fully remove the BSSE (that could have been done by introducing ghost atoms), but substantially cancels systematic errors.

3.1 SIESTA calculations for single adsorbed atoms (Na and K)

A smooth variation of the total energy and magnetic moment on approaching an alkali metal atom (K and Na have been tested) to the BC₃ sheet (without performing any structure relaxation and only converging the electronic structure) is depicted in Figure 1. For the record, the lattice parameter in these trial calculations done with SIESTA was fixed at $a = 5.170 \text{ \AA}$. The idea of this exercise was to inspect the sharpness of the potential energy minimum, and, in the case of Na, to test the stability of results against the choice of pseudopotential, in the construction of which the arguments could have been found to explicitly include the semicore Na $2p$ states among the “valence” ones, or attribute them to the core. As can be concluded from Figure 1 (right panel), the difference in the potential energy profiles stemming from these two choices is acceptably small yet noticeable. For the subsequent study of Na–Na interactions, we “pragmatically” opted for using the “small core” Na pseudopotential with $2p$ treated as valence state. This choice results in more accurate estimation of equilibrium atom-to-monolayer distance and yields a better pronounced discrimination between the adsorption energies of Na and K atoms, which seems to be consistent with general trend found by other calculations listed in Table 2 (whatever would be the sources of error in reported *absolute* energy values). The depth of the total energy profile gives a fair estimate of the adsorption energy. The magnetic moment exhibits instability throughout the range of distances 3 to 7 Å for K, or 5 to 8 Å for Na, as the outer s state of the corresponding alkali metal, which carries an unpaired spin in a free atom, starts to interact with the wavefunctions of the BC₃ layer. The corresponding part is therefore not shown in the magnetic moment plots in Figure 1. Upon adsorption and after atomic and electronic relaxation, the magnetic moment is fully dissolved (differently e.g. from the situation with graphene, on which the adsorbed K atom retains its magnetic moment).¹

The results obtained in the course of relaxing atomic positions within a supercell of a fixed size, corresponding to the lattice parameter $a = 5.17 \text{ \AA}$ (as optimized in QE calculation), by comparing the total energies from “adsorbed atom” and “distant atom” situations within the same calculation setup, are shown in Table 2. For comparison, using as reference values the total energies of the BC₃-only supercell and the “single-atom-only” supercell instead of the “BC₃ plus distant atom” one yields the adsorption energies of $\simeq 2.1 \text{ eV}$, for the case of potassium.

¹The asymptotic value of the magnetic moment corresponding to large distances in Figure 1 does not reach $1 \mu_B$ – probably due to a purely technical drawback that very fine \mathbf{k} and energy mesh is needed to cope with very narrow s -states energy levels.

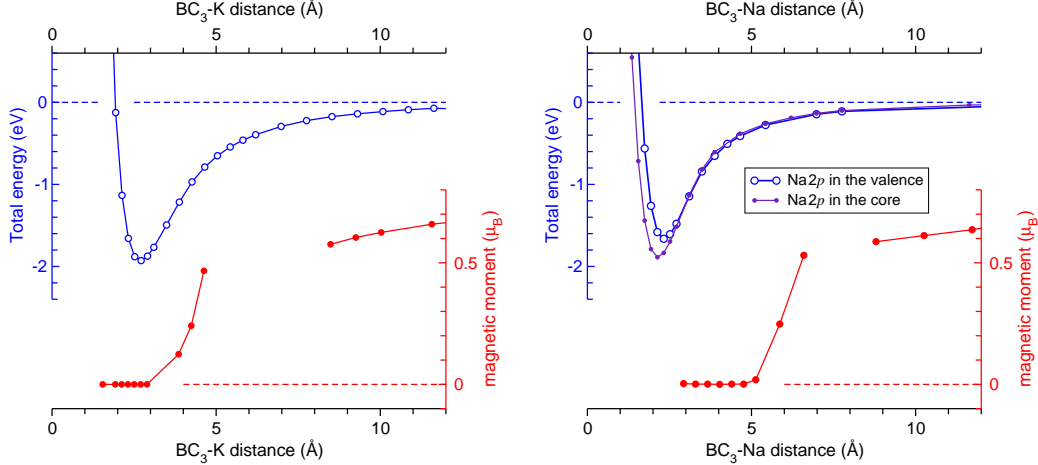


Figure 1: Total energy (upper plots, blue curves, axes on the left) and magnetic moment (lower plots, red dots, axes on the right) as functions of the height of the alkali metal atom (left panel: K, right panel: Na) over the BC_3 layer. Calculations are done with lattice constant fixed at $a = 5.17 \text{ \AA}$ without structure relaxation. For Na, the results are shown for two norm-conserving pseudopotentials, for the cases of $\text{Na}2p$ states treated as valence states or attributed to the core. See text for details.

3.2 Adsorption energies calculated with QE; role of dispersion interactions

Independently, we calculated the adsorption energy of $M=(\text{Li}, \text{Na}, \text{K})$ atoms at HC, HB and AB sites by the QE method, also for the $3 \times 3 \times 1$ supercell, referring in this case to the total energy differences of the kind (Supercell with adsorbed M) - [(Supercell without M) + (Single M atom in the box)], which approach is less problematic when using a planewave-basis code not prone to BSSE. In view of expected non-negligible effect of dispersion interactions (not included in conventional PBE calculations) on the adsorption

Table 2: Calculated parameters of alkali metal atoms adsorbed at C_6 hollow site of BC_3 . E_a : adsorption energy (defined positive, i.e., corresponding to energy gain on adsorption, in all cases); h : the height of the adsorbed atom over the BC_3 plane. See text for detail.

Method	Ref.	Supercell	E_a (eV)			h (\AA)		
			Li	Na	K	Li	Na	K
OpenMX or SIESTA (GGA) [†]	[9]	$2 \times 2 \times 1$	0.81	1.34	0.82	2.31	2.23	2.57
VASP (GGA) [†]	[8]	$2 \times 2 \times 1$	5.13	4.47	4.72	1.74	2.15	2.53
VASP (GGA) [†]	[5]	$3 \times 3 \times 1$	1.26	1.16	1.75	1.77	2.18	2.58
SIESTA (GGA)	present work*	$3 \times 3 \times 1$		1.53	1.66		2.18	2.68
QE (GGA) [‡]	present work*	$3 \times 3 \times 1$	2.56	1.85	2.31	1.73	2.26	2.63

[†]with Grimme-D2; [‡]for results with Grimme-D2 correction, see next table. * $a=5.17 \text{ \AA}$ fixed.

Table 3: Adsorption energy (defined positive for energy gain) and height over BC_3 layer for Li, Na and K atoms in three symmetric positions, according to QE calculations with PBE (upper line in each block for a given atom) and with Grimme-D2 correction included (lower line; the value in parentheses gives the difference with respect to the PBE value).

	Adsorption energy (eV)			Height over layer (\AA)		
	HC	HB	AB	HC	HB	AB
Li	2.56	2.47	2.09	1.73	1.72	1.91
	2.91 (+0.36)	2.85 (+0.39)	2.41 (+0.32)	1.80 (+0.08)	1.73 (+0.06)	1.73 (-0.18)
Na	1.85	1.83	1.69	2.26	2.22	2.28
	2.23 (+0.38)	2.22 (+0.40)	2.02 (+0.33)	2.28 (+0.02)	2.23 (+0.01)	2.23 (-0.05)
K	2.31	2.25	2.20	2.63	2.62	2.65
	2.61 (+0.29)	2.56 (+0.30)	2.48 (+0.28)	2.63 (+0.00)	2.62 (+0.00)	2.58 (-0.07)

characteristics, we simulated it (the effect) on the total energy within broadly used semiempirical Grimme’s G2 correction[10]; the equilibrium geometries were affected accordingly. The results (adsorption energies and equilibrium heights of adsorbed atoms over the BC_3 plane) are shown in Table 3, the net effect of the G2 correction to the GGA results being placed in brackets.

The calculated adsorption energy values are consistent with those from the recent work by Zhao *et al.*[5] by the order of magnitude and in an observation that the adsorption at HC and HB sites is very competitive (being in all cases stronger in HC), both corresponding energies being larger than that at the AB site. The exact values are systematically, albeit slightly, larger in our QE calculation. We note in passing that the calculated adsorption energies reported by Naqvi *et al.*[8] are largely overestimated by roughly a factor of two while those reported by Bafekry *et al.*[9] are largely, and unevenly, underestimated.

We note however that the variation of adsorption energies over different adsorption sites, which is the smallest ($\simeq 0.13$ eV) for K, larger ($\simeq 0.2$ eV) for Na and the largest ($\simeq 0.5$ eV) for Li, is in perfect agreement between our study and Ref. [5] (see Figure 5 therein). This may be due to the fact that systematic errors potentially present in calculations of adsorption energies by this or that method are practically cancelled in the estimation of “barrier heights” between adsorption sites.

The equilibrium positions of adsorbed atoms over the monolayer are in excellent agreement with almost all previous calculations (see Table 2). As is seen from Table 3, equilibrium distances are in general only weakly affected by inclusion of the Grimme’s correction, hence probably more “reliable” and reproducible character of these calculated values.

The hence discussed relations between energies of different species at different adsorption sites underline a special standing of potassium among alkali metal atoms in that its potential energy landscape over the BC_3 layer is particularly flat, which may imply a good mobility. This comes with an appreciable adsorption energy, so – simplifying – potassium easily sticks to BC_3 and easily rolls over it.

In the next section, we come to the analysis of interaction between adsorbed alkali metal atoms.

4 Interaction of alkali metal atoms adsorbed on BC_3

4.1 Spatial map of $M-M$ interaction energies on the BC_3 surface

In order to gain a substantial and reliable information concerning the interaction between alkali metal atoms M adsorbed on BC_3 (specifically, Na and K have been studied), we staged a series of simulations on large supercells containing two adsorbed atoms. One of them, the “reference atom”, was placed in a (lowest-energy) HC position over the center of a C_6 ring, and the other, “trial” atom – at different local-minima positions at different distances from the reference atom. Within the 5×5 supercell (200 atoms), all non-equivalent adsorption positions have been explored within the “irreducible wedge” (shown in inset of Figure 2) closest to a given HC site. This amounted to four HC positions, 9 HB positions (over the center of C_4B_2 hexagons) and 7 AB positions (atop of a boron atom), hence the positions

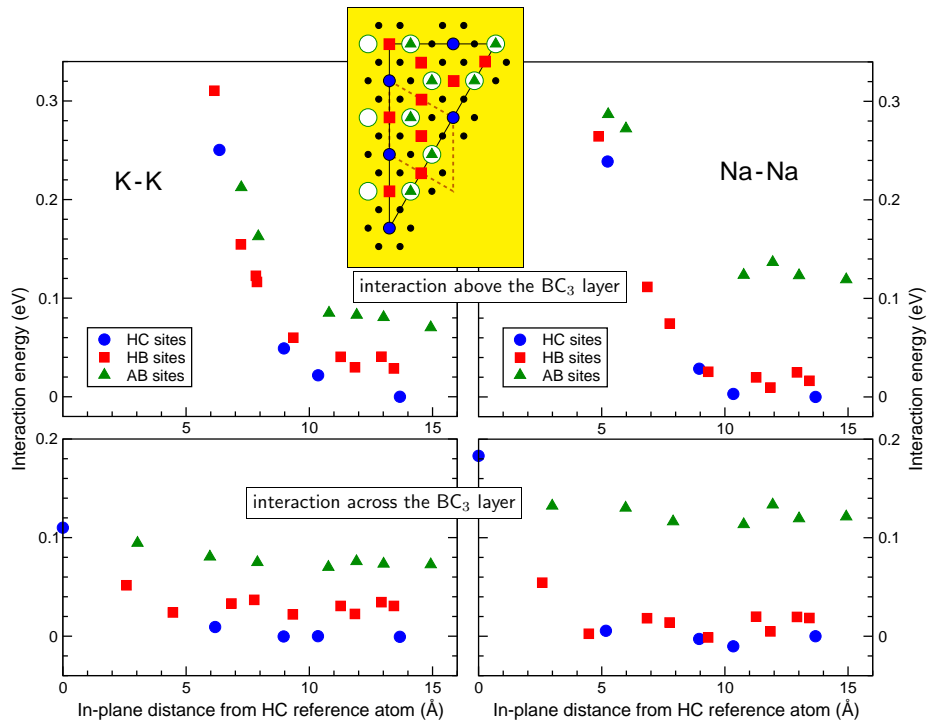


Figure 2: Map of interaction energies between alkali metal atoms (two panels on the left refer to K–K, two on the right to Na–Na), adsorbed at different sites of the BC_3 lattice (marked by circles, squares and triangles in the “irreducible part” of the 5×5 supercell schematically shown in the inset), and the reference atom in the HC position (the bottom blue point in the inset). HC positions (over C_6 hexagons), HB positions (over C_4B_2 hexagons) and AB positions (over B atoms) are indicated by different symbols. The two upper panels refer to the interactions between atoms adsorbed at the same side of the BC_3 plane, the bottom panels – between atoms adsorbed at the opposite sides, in both cases – as function of the in-plane distances between the adsorption sites. Positions included in the mapping are marked by symbols, as in the main plot. A primitive cell of BC_3 is outlined by a dashed contour in the inset.

confirmed (see previous Section) to correspond to stable (local energy minima) adsorption sites. Moreover, the configurations in which the second (trial) atom was adsorbed at the *opposite* side of the BC_3 monolayer have been tested – on all the HC, HB and AB sites, mentioned above, plus directly at the reference site, in a mirror position from the reference atom. In all cases, an unconstrained relaxation has been performed (fixing however the supercell parameters), which yielded the total energy and the equilibrium geometry.

For M – M distances starting from $\sim 7\text{\AA}$ onwards, the relaxation patterns are barely visible: the adsorbed atoms reside in their nominal positions, so that only tiny modifications of interatomic distances come about. The BC_3 layer in all cases looks extremely rigid and planar, without a marked tendency towards bending or warping. At shorter distances, the repulsion between the adsorbed atoms pushes them out of symmetry positions; the examples of this will be discussed below. In fact, the stabilisation of the trial atom in the nearest HB or AB position to the reference atom becomes impossible, because the atoms drift away from such configuration. This refers to the atoms adsorbed at the same side of the BC_3 plane. The atoms adsorbed “across the plane” remain practically insensitive to the closeness of the reference atom, exhibiting no perturbations in their relaxation pattern, and the energies which are largely independent on the in-plane distance to the reference atom.

The “interaction energies” plotted in Figure 2 are defined as total energies from each calculations, expressed relative to the energy of supercell in which the two atoms are at maximally separated HC positions, within the given type of placement (i.e., either both above, or one below the BC_3 layer), effectively setting the “infinity limit” within the given supercell size. We note that these “infinity limit” energies are not exactly equal for the trial atom being on the same side of the BC_3 plane as the reference atom, or on the opposite side. In fact, the second energy is lower by 0.03 eV for Na adsorption and by 0.05 eV for K adsorption. This disparity (which would disappear be the atoms at really sufficiently far distance) can be considered as a measure of the effect of our limited supercell size.

Choosing such “distant M – M ” limit of two adsorbed atoms as the reference level leaves the *adsorption energy* at a HC site out of our grasp; however, this issue has been separately addressed in the previous section. However, the *differences* between adsorption energies at HC, HB and AB sites, or otherwise the barrier heights, are easily readable from Figure 2, and are instructive to discuss.

We note first that for “inverted” adsorption of a trial atom (cf. bottom panels in Figure 2), the energy of its interaction with the reference one is practically independent on interatomic distance, and follows the universal trend that HB positions are, on the average, higher in energy by $\simeq 0.03$ eV than the HC ones, whereas the AB positions are higher than the HC by $\simeq 0.08$ eV, in case of K adsorption. As for the Na adsorption, the energies at HC and HB positions are almost identical within the “numerical noise”, the HB ones being just a bit higher, whereas the energies in AB positions are much higher, by $\simeq -0.12$ eV. This simply passes the information about barrier heights (differences between adsorption energies at different sites), which was already addressed in the previous section, see e.g. Table 3. However, here it appears not as a “random” number but as a “statistically credible” result. We can again refer to the similarity of the present estimation of barrier heights with those given by Zhao *et al.* [5], notably in Figure 5(c,d) of this publication.

The bottom panel of Figure 2 suggests that the alkali metal atoms “do not see each other” across the BC_3 plane till the M – M distance becomes really short, within the closest

adsorption sites. Still, this does not bring about neither an “asymmetric” relaxation nor noticeable augmentation of the z -coordinate; the adsorbed atoms remain well centered at their respective sites. The “double occupation” of a HC adsorption site from both sides of the BC_3 plane, whereby the two K atoms remain stable at a distance 5.4 \AA (hence at a regular height above the layer) is by far not so energetically unfavourable as it could have been *a priori* anticipated; it costs only 0.1 eV to bring a K atom from a distant HC site onto this “antipode” reference site; for Na atoms the corresponding energy is 0.18 eV .

The established hierarchy of barrier heights, revealed via interaction energies being independent on the M - M distance, is also valid for adsorptions at the same side of the BC_3 plane (see upper panels of Figure 2), provided the M atoms are placed not closer than $\simeq 10 \text{ \AA}$. At shorter distances, the energy barrier rapidly increases, forming a nearly rigid core of the radius of $\simeq 5 \text{ \AA}$ for Na and $\simeq 6 \text{ \AA}$ for K, irrespectively of the adsorption site concerned.

4.2 Unusual relaxation patterns of closely placed adsorbed atoms

The placement of trial atoms at adsorption sites close (within $\simeq 8 \text{ \AA}$) of the reference atom resulted in a noticeable repulsion of both atoms in their relaxed configurations, as shown in Figure 3 for the case of potassium. The reference atom displaces in its “nest” over the C_6 ring without however leaving the latter, whereas the trial atom could have been pushed from its initial “on top of B” position onto that above the C-B bond; see the case AB in Figure 3. It was not possible to stabilise the trial atoms in AB or HB positions closest to the reference atom, since the interacting atoms were pushed apart into “second-neighbours” configurations, shown in Figure 3. This strengthens an idea of “hard core” repulsion potential which effectively prevents the potassium atoms to come closer than about 6 \AA . This minimal distance corresponds to both atoms residing over the second-neighbour C_6 - C_6 or C_6 - C_4B_2 hexagons, slightly pushed apart from the respective centers, as shown in Figure 3. We note that the z -coordinates of potassium atoms are not much affected by their relaxation “situation”; also the warping of the BC_3 layer, although noticeable around

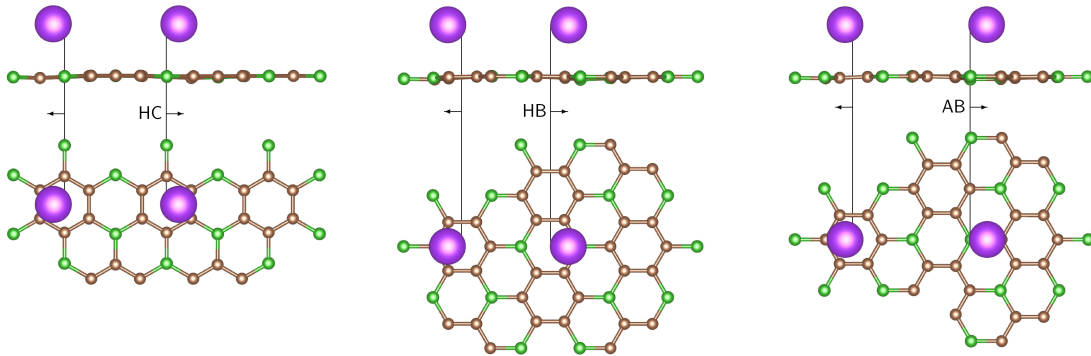


Figure 3: Three relaxed structures (top row: side views, bottom row: top views) of trial K atoms initially placed at HC, HB and AB positions close to the reference K atom (that in the left of each plot). The arrows indicate the movement of the both K atoms apart.

5 Conclusion

Summarizing, we found that alkali metal atoms, sodium and potassium, adsorbed over the BC₃ monolayer interact strongly repulsively at distances smaller than $\simeq 10$ Å, and otherwise remain relatively insensitive to the mutual presence, feeling the “usual” landscape of potential barriers of $\lesssim 0.1$ eV (case of K) or $\lesssim 0.15$ eV (case of Na) in their movement over the BC₃ plane. A combination of relatively high adsorption energy with respectively low barriers, especially prominent for potassium, known already from early works, suggested already an interesting interplay of sticking and mobility. Now we conclude that even relatively high concentration of adsorbed K atoms might not prevent them from acting as a highly mobile “gas” on the BC₃ surface. This may open perspectives for further more realistic simulations and interesting applications.

Supporting Information

which includes tables with (relaxed) interatomic distances and energies for all the adsorption sites (the data depicted in Figure 2) is available from the Wiley Online Library or from the authors.

References

- [1] H. Tanaka, Y. Kawamata, H. Simizu, T. Fujita, H. Yanagisawa, S. Otani, C. Oshima, *Solid State Communications* **2005**, *136*, 1–22.
- [2] Y. Qie, J. Liu, S. Wang, S. Gong, Q. Sun, *Carbon* **2018**, *129*–38.
- [3] S. Mehdi Aghae, M. M. Monshi, I. Torres, S. M. J. Zeidi, I. Calizo, *Applied Surface Science* **2018**, *427*–326.
- [4] S. Aydin, M. Şimşek, *International Journal of Hydrogen Energy* **2019**, *44*, 14–7354.
- [5] L. Zhao, Y. Li, G. Zhou, S. Lei, J. Tan, L. Lin, J. Wang, *Chinese Chemical Letters* **2020**, *32*, 2–900.
- [6] J. P. Perdew, K. Burke, M. Ernzerhof, *Phys. Rev. Lett.* **1996**, *77*, 18–3865.
- [7] J. P. Perdew, K. Burke, M. Ernzerhof, *Phys. Rev. Lett.* **1997**, *78*, 7–1396.
- [8] S. R. Naqvi, T. Hussain, S. R. Gollu, W. Luo, R. Ahuja, *Applied Surface Science* **2020**, *512*–145637.
- [9] A. Bafekry, S. Farjami Shayesteh, M. Ghergherehchi, F. M. Peeters, *Journal of Applied Physics* **2019**, *126*, 14–144304.
- [10] S. Grimme, *Journal of Computational Chemistry* **2006**, *27*, 15–1787.
- [11] P. Giannozzi, S. Baroni, N. Bonini, M. Calandra, R. Car, C. Cavazzoni, D. Ceresoli, G. L. Chiarotti, M. Cococcioni, I. Dabo, A. Dal Corso, S. de Gironcoli, S. Fabris, G. Fratesi, R. Gebauer, U. Gerstmann, C. Gougoussis, A. Kokalj, M. Lazzeri, L. Martin-Samos, N. Marzari, F. Mauri, R. Mazzarello, S. Paolini, A. Pasquarello, L. Paulatto, C. Sbraccia, S. Scandolo, G. Sclauzero, A. P. Seitsonen, A. Smogunov,

- P. Umari, R. M. Wentzcovitch, *Journal of Physics: Condensed Matter* **2009**, *21*, 39 395502.
- [12] P. Giannozzi, O. Andreussi, T. Brumme, O. Bunau, M. Buongiorno Nardelli, M. Calandra, R. Car, C. Cavazzoni, D. Ceresoli, M. Cococcioni, N. Colonna, I. Carnimeo, A. Dal Corso, S. de Gironcoli, P. Delugas, R. A. DiStasio Jr, A. Ferretti, A. Floris, G. Fratesi, G. Fugallo, R. Gebauer, U. Gerstmann, F. Giustino, T. Gorni, J. Jia, M. Kawamura, H.-Y. Ko, A. Kokalj, E. Küçükbenli, M. Lazzeri, M. Marsili, N. Marzari, F. Mauri, N. L. Nguyen, H.-V. Nguyen, A. Otero-de-la Roza, L. Paulatto, S. Poncé, D. Rocca, R. Sabatini, B. Santra, M. Schlipf, A. P. Seitsonen, A. Smogunov, I. Timrov, T. Thonhauser, P. Umari, N. Vast, X. Wu, S. Baroni, *Journal of Physics: Condensed Matter* **2017**, *29*, 46 465901.
- [13] J. M. Soler, E. Artacho, J. D. Gale, A. García, J. Junquera, P. Ordejón, D. Sánchez-Portal, *Journal of Physics: Condensed Matter* **2002**, *14*, 11 2745.
- [14] A. García, N. Papior, A. Akhtar, E. Artacho, V. Blum, E. Bosoni, P. Brandimarte, M. Brandbyge, J. I. Cerdá, F. Corsetti, R. Cuadrado, V. Dikan, J. Ferrer, J. Gale, P. García-Fernández, V. M. García-Suárez, S. Garcí, G. Huhs, S. Illera, R. Korytár, P. Koval, I. Lebedeva, L. Lin, P. López-Tarifa, S. G. Mayo, S. Mohr, P. Ordejón, A. Postnikov, Y. Pouillon, M. Pruneda, R. Robles, D. Sánchez-Portal, J. M. Soler, R. Ullah, V. W.-z. Yu, J. Junquera, *The Journal of Chemical Physics* **2020**, *152*, 20 204108.
- [15] N. Troullier, J. L. Martins, *Phys. Rev. B* **1991**, *43* 1993.
- [16] I. V. Zaporotskova, S. V. Boroznin, *Modern Electronic Materials* **2017**, *3*, 2 91.
- [17] B. Mortazavi, M. Shahrokhi, M. Raeisi, X. Zhuang, L. F. C. Pereira, T. Rabczuk, *Carbon* **2019**, *149* 733.
- [18] S. F. Boys, F. Bernardi, *Molecular Physics* **1970**, *19* 553.